Long-lived states of methylene protons in achiral molecules

Anna Sonnefeld, Aiky Razanahoera, Philippe Pelupessy, Geoffrey Bodenhausen, Kirill Sheberstov

CHEMICAL PHYSICS

Long-lived states of methylene protons in achiral molecules

Anna Sonnefeld, Aiky Razanahoera, Philippe Pelupessy, Geoffrey Bodenhausen, Kirill Sheberstov*

In nuclear magnetic resonance (NMR), the lifetimes of long-lived states (LLSs) are exquisitely sensitive to their environment. However, the number of molecules where such states can be excited has hitherto been rather limited. Here, it is shown that LLSs can be readily excited in many common molecules that contain two or more neighboring CH_2 groups. Accessing such LLSs does not require any isotopic enrichment, nor does it require any stereogenic centers to lift the chemical equivalence of CH_2 protons. LLSs were excited in a variety of metabolites, neurotransmitters, vitamins, amino acids, and other molecules. One can excite LLSs in several different molecules simultaneously. In combination with magnetic resonance imaging, LLSs can reveal a contrast upon noncovalent binding of ligands to macromolecules. This suggests new perspectives to achieve high-throughput parallel drug screening by NMR.

INTRODUCTION

In nuclear magnetic resonance (NMR), the memory of spin systems is normally limited by longitudinal relaxation. However, long-lived states (LLSs) have lifetimes T_{LLS} that can be substantial longer than T_1 (*1*–*3*). The discovery of LLSs and the invention of methods to excite them have opened new perspectives, in particular for revealing interactions between potential drugs and target proteins (*4*–*6*), for the observation of hyperpolarized metabolites (*7*–*10*), for probing slow chemical exchange (*11*), for determining rates of slow diffusion (*12*, *13*), for storing nuclear hyperpolarization (*14*–*17*), for selecting signals of interest in peptides and proteins (*18*, *19*), and for detecting signals of metabolites in magnetic resonance imaging (MRI) (*19*–*22*).

In molecules with two magnetically equivalent spins, such as in gaseous hydrogen H_2, the population of the singlet state αβ-βα of the two proton spins can be enhanced with respect to its thermal equilibrium, thus giving rise to a singlet-triplet population imbalance ΔP_{STI}. This imbalance can persist for a long lifetime T_{LLS} because the conversion of populations between the singlet and triplet manifolds is forbidden by symmetry. In molecules with CH_2 groups, a population imbalance ΔP_{STI} between the singlet and triplet manifolds of the two protons can be readily excited when the chemical equivalence of the two nuclei is lifted, i.e., when they have distinct chemical shifts (*23*). This occurs for diastereotopic pairs of protons in chiral molecules, where the degeneracy of the chemical shifts is lifted by the presence of (possibly remote) stereogenic centers (*24*, *25*). The larger the difference in chemical shift between the protons of a methylene group, the greater the "leakage" of population between singlet and triplet states, thus resulting in shorter lifetimes T_{LLS}. This effect can be attenuated by shuttling the sample to low fields or by "sustaining" the LLS by strong radio-frequency (RF) irradiation at high fields. Both approaches suffer from obvious disadvantages.

This paper shows that one can also create LLSs involving two methylene protons that are chemically equivalent (i.e., having identical chemical shifts), provided that they are magnetically inequivalent, i.e., having distinct scalar couplings to other nuclei, such as the protons of nearby CH_2 groups. A similar approach was demonstrated previously for magnetically inequivalent ^{13}C and ^{15}N spin pairs (*26*–*31*) and for pairs of protons coupled to deuterium (*32*), but this requires isotopic enrichment. Pairs of geminal protons in CH_2 groups are good candidates for supporting population imbalances with long lifetimes, since the intrapair dipole-dipole interaction does not cause any relaxation of their singlet-triplet population imbalance. Singlet-triplet imbalances are further "protected" against coherent dissipation by geminal *J*-couplings (*33*), which lift the degeneracy between the singlet and the central triplet states. Therefore, LLSs in magnetically inequivalent CH_2 groups do not require any external manipulations to be sustained, as was confirmed for all molecules with LLSs studied in this work.

To use LLSs as sensors for binding in drug screening, one must be able to excite LLSs in a broad range of potential drug molecules. The ability to use magnetic inequivalence in aliphatic segments greatly increases the number of potential ligands that can be screened. Accelerating the throughput of drug screening requires methods for parallel detection (*34*) or MRI of bundles of capillaries (*35*). Proof-of-principle experiments illustrating this idea are presented in this work.

There are several approaches to create LLSs in strongly coupled spin pairs, including magnetization-to-singlet (M2S) sequence (*24*, *36*) and symmetry-based pulse sequences (*37*). More specific pulse sequences were developed to transfer singlet order from strongly coupled protons enhanced by para-hydrogen to a heteronucleus such as ^{13}C (*38*–*41*). We believe that spin-lock–induced crossing (SLIC) (*25*, *42*–*44*) and polychromatic variants (poly-SLIC) (*45*) are the most appropriate methods for exciting LLSs in methylene protons, as discussed below.

RESULTS

A selection of common molecules with aliphatic chains where LLSs can be excited by SLIC is shown in Fig. 1. The optimum SLIC parameters and relaxation properties are summarized in Table 1. The conditions for LLS excitation are similar for all compounds so that several independent LLSs can be excited simultaneously in mixtures of molecules with aliphatic chains.

Excitation of singlet states in methylene chains

A spin system with two magnetically inequivalent CH_2 groups can be classified as $AA'XX'$ in Pople's notation (*46*). Magnetic inequivalence

Department of chemistry, École Normale Supérieure, PSL University, Paris, France.
*Corresponding author. Email: kirill.sheberstov@ens.psl.eu

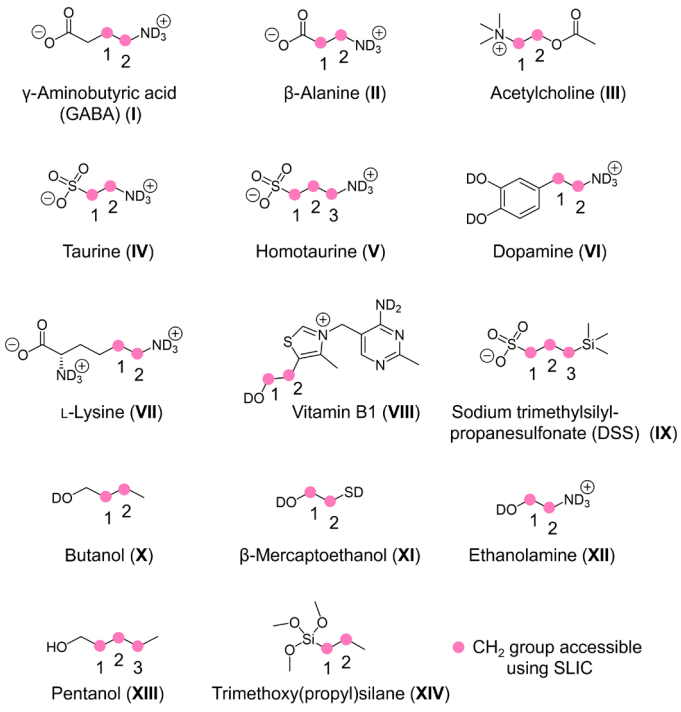

Fig. 1. A selection of common molecules with methylene groups where LLS can be excited. The CH_2 groups that were experimentally found to be accessible for excitation of LLSs by SLIC are emphasized in pink. In the case of (chiral) lysine (**VII**), the diastereotopic β and γ CH_2 groups feature distinct chemical shifts, so that LLSs can be excited by a variety of methods, while the protons of the δ and ε CH_2 groups have nearly degenerate chemical shifts, where LLSs can be best excited by SLIC. With the exception of pentanol (**XIII**) and trimethoxy(propyl)silane (**XIV**), all compounds were measured in D_2O.

between the protons of a methylene group is due to differences between the vicinal out-of-pair *J*-couplings. These couplings obey Karplus-type equations with coefficients that depend on functional groups and solvent properties (*47*, *48*). Except in rare cases where all three rotamer populations are equal, the population-weighted averages of the vicinal *J*-couplings are unequal, i.e., ${}^3J_{AX} = {}^3J_{A'X'} \neq {}^3J_{AX'} = {}^3J_{A'X}$.

This makes it possible to populate LLSs using SLIC. The optimum RF amplitude (nutation frequency) ν_1^{SLIC} and duration τ_{SLIC} of the SLIC pulse depend on only two parameters

$$\begin{aligned} 2J_{intra} &= {}^2J_{AA'} + {}^2J_{XX'} \\ \Delta J &= {}^3J_{AX} - {}^3J_{AX'} \end{aligned} \quad (1)$$

The RF amplitude should match the sum of intrapair *J*-couplings $2J_{intra}$, while the duration should be inversely proportional to the difference between the out-of-pair couplings Δ*J*

$$\begin{aligned} \nu_1^{SLIC} &= |2J_{intra}| \\ \tau_{SLIC} &= 1/(\sqrt{2} \cdot |\Delta J|) \end{aligned} \quad (2)$$

A single-SLIC pulse must be applied on resonance with the chemical shift of the CH_2 group of interest. Poly-SLIC can be used to irradiate several CH_2 groups in the same molecule simultaneously. The optimum conditions of the SLIC pulse are different in this case, requiring a weaker amplitude $\nu_1^{poly-SLIC} = |J_{intra}|$ and a longer duration $\tau_{poly-SLIC} = 1/|\Delta J|$ (*45*).

The parameters for SLIC pulses with a single RF were optimized for all 14 molecules in Fig. 1, as reported in Table 1. The optimum RF amplitudes $25 \leq \nu_1^{SLIC} \leq 29$ Hz are similar for all compounds, since the geminal two-bond *J*-couplings lie within a narrow range of $12.5 \leq |{}^2J| \leq 14.5$ Hz. The optimum pulse durations vary over a broader range of 110 ms $\leq \tau_{SLIC} \leq$ 845 ms. In the case of β-mercaptoethanol, where the optimum duration is τ_{SLIC} = 845 ms, this reflects the small difference Δ*J* = 0.8 Hz. In this case, it is not immediately apparent from the conventional spectrum that one is dealing with an *AA'XX'* rather than an A_2X_2 system. The closer the systems are to magnetic equivalence, the more the multiplets take on the appearance of triplets with a binomial 1:2:1 intensity distribution. Nevertheless, the CH_2 protons in β-mercaptoethanol, taurine, and β-alanine can be addressed by SLIC. The Supplementary Materials show that the difference between the chemical shifts of the *AA'* and *XX'* spins should be at least 60 Hz [0.1 parts per million (ppm) at 500 MHz] for LLS excitation. For aliphatic chains comprising three or more methylene groups, at least one of them should have a distinct chemical shift, as we observed in the case of pentanol.

The LLSs created by SLIC are delocalized, since RF irradiation at the chemical shift of a selected CH_2 group also excites LLSs associated with one to two neighboring CH_2 groups (*45*). Superpositions of LLSs in aliphatic chains involving more than four spins can have several relaxation rates (*45*, *49*). However, all experimental decays observed in this work could be fitted with monoexponential decays. The Supplementary Materials show that a unique state is excited in *AA'XX'* systems in molecules with two pairs of CH_2 protons, in contrast to longer chains (*45*), and that the yields of the excitation and reconversion of the LLS can be expressed in analytical form.

Rotational conformers and magnetic inequivalence

In aliphatic chains comprising adjacent CH_2 units, the parameter Δ*J* (and hence the optimum duration τ_{SLIC}) reflects the fact that the populations of rotamers are not equal. These populations can be affected by the following factors:

1) Steric hindrance between bulky groups can cause one of the rotational conformers to be preferred. Compounds with small substituents and short aliphatic chains or weak intramolecular interactions are therefore less likely to have accessible LLSs. For example, no LLS could be excited by SLIC in propanol, but all CH_2 groups in butanol (**X**) and pentanol (**XIII**), except for their CH_2OH groups, have accessible LLSs.

2) Electrostatic interactions between charged groups can stabilize one of the rotational conformers, thus granting access to the LLS. At neutral pH, only two of the three CH_2 groups in γ-aminobutyric acid (GABA) were accessible. At pH 12, all three methylene groups become accessible.

3) If a compound contains H-bond donors and acceptors, some rotational conformers can be stabilized by intramolecular H-bonds.

The relation between Δ*J* and the populations of rotamers is discussed in the Supplementary Materials. For the smallest Δ*J* value of 0.8 Hz that we could exploit to excite LLSs by SLIC, the deviation from equal rotamer populations must be at least 7%, whereas for the largest observed Δ*J* value of 6.5 Hz, it is estimated to be as large as 80%. Here, 100% corresponds to the limit where only the anti rotamer would be populated.

Table 1. Optimized SLIC parameters and relaxation properties of the studied molecules. Unless otherwise specified, all compounds were measured in D_2O. Unless specified otherwise, the pH was controlled using a phosphate buffer adjusted to neutral pH.

Molecule	Number	ν_1^{SLIC} (Hz)	τ_{SLIC} (ms)	Irradiated CH_2 (Fig. 1)	T_1 (s)	T_{LLS} (s)	T_{LLS}/T_1
γ-Aminobutyric acid (GABA)	I	26	220	1	1.8	11.7	6.5
				2	2.0	10.5	5.3
β-Alanine	II	29	540	1	3.1	17.1	5.5
				2	3.1	17.4	5.6
Acetylcholine	III	29	120	1	2.0	5.8	2.9
				2	2.2	5.7	2.6
Taurine	IV	28	520	1	3.2	19.3	6.0
				2	3.3	17.8	5.4
Homotaurine	V	26	180	1	2.3	8.1	3.5
				2	2.3	10.6	4.6
				3	2.5	8.6	3.4
Dopamine	VI	27	500	1	0.7	3.9	5.3
				2	0.8	4.2	5.6
L-lysine	VII	27	205	1	0.8	2.9	3.6
				2	1.0	2.8	2.8
Vitamin B1*	VIII	26	250	1	0.9	6.0	6.7
				2	0.9	5.6	6.2
DSS	IX	27	110	1	1.7	7.0	4.1
				2	1.7	8.4	4.9
				3	1.7	7.6	4.5
Butanol	X	25	200	1	3.6	12.5	3.5
				2	3.9	14.7	3.8
β-Mercaptoethanol	XI	25	845	1	5.6	25.4	4.5
				2	5.7	25.8	4.5
Ethanolamine	XII	25	190	1	2.5	12.1	4.8
				2	2.5	12.3	4.9
Pentanol†	XIII	26	190	1	4.6	6.5	1.4
				2	3.8‡	–‡	–‡
				3	3.8‡	–‡	–‡
Trimethoxy(propyl)-silane†	XIV	28	125	1	3.5	8.0	2.3
				2	3.9	7.3	1.9

*Measured in D_2O without buffer to control the pH. †Measured in $CDCl_3$. ‡Spectral overlap prevented the determination of individual T_1 and T_{LLS} values.

Polychromatic SLIC applied to mixtures

The poly-SLIC approach can be applied to observe LLSs simultaneously in different molecules in a mixture. Figure 2A shows a conventional NMR spectrum of a mixture containing sodium trimethylsilyl-propanesulfonate (DSS), ethanolamine, β-alanine, taurine, and GABA. Figure 2B shows a spectrum of the same mixture after excitation of LLSs and reconversion into observable magnetization using a superposition of five poly-SLIC pulses with a common RF amplitude $\nu_1^{SLIC} = 27$ Hz and a common duration $\tau_{SLIC} = 319$ ms. Within each molecule, only one methylene group was irradiated. The integrated intensities of the signals varied between 0.5 and 1.2% of their amplitudes in the conventional spectrum for an LLS relaxation interval of $\tau_{rel} = 3$ s. In such a mixture, the RF amplitude and duration of SLIC pulses cannot be optimized simultaneously for all compounds. For β-alanine, the signal was weak because ν_1^{SLIC} and τ_{SLIC} deviated from their optimum values. Although the LLSs were created with relatively low yields, the signal-to-noise ratio was sufficient with eight scans at 10 mM concentrations.

When using optimized SLIC parameters, typical LLS-derived integrated signal intensities for monochromatic SLIC were ca. 5% of the integrated signal intensity in a conventional one-dimensional (1D) spectrum. Theory predicts that single-SLIC excitation and reconversion pulses in a four-spin system can provide a maximum yield of 14% of the magnetization of the irradiated spin pair. For

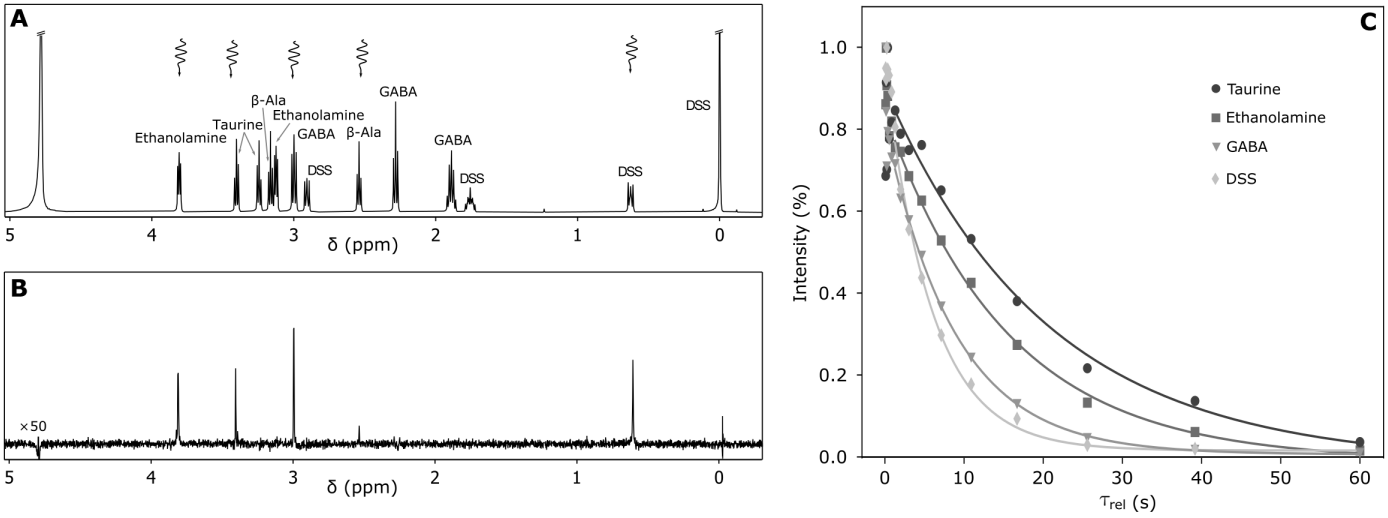

Fig. 2. Simultaneous observation of LLSs in a mixture. The mixture contained ca. 10 mM ethanolamine, taurine, β-alanine, GABA, and DSS in a 50 mM phosphate buffer in D_2O. (**A**) Conventional ^1H NMR spectrum of the mixture acquired with eight scans. (**B**) Spectrum acquired after a poly-SLIC sequence with five RFs indicated by wavy arrows in (A), with eight scans and an LLS relaxation interval τ_{rel} = 3 s. The spectrum is scaled by a factor of 50 with respect to (A). (**C**) LLS decays of four molecules measured simultaneously. The LLS lifetimes were determined from monoexponential fits, ignoring weak initial oscillations that can be neglected after τ_{rel} > 1.3 s: T_{LLS} (taurine) = 20.6 ± 2.3 s, T_{LLS} (ethanolamine) = 14.1 ± 0.7 s, T_{LLS} (GABA) = 8.9 ± 0.3 s, and T_{LLS} (DSS) = 5.9 ± 0.5 s.

double-SLIC excitation, we typically observed LLS-derived integrated signal intensities of ca. 10%. The Supplementary Materials show that for double-SLIC applied to two neighboring CH_2 groups, the theoretical yield can reach 28% of the total magnetization. By using unitary constraints (*50*) adapted to take spin symmetry into account (*51*), one can verify that this corresponds to the maximum yield after excitation and reconversion.

In Fig. 2B, only signals that stem from LLSs are observed. All other peaks are removed from the spectrum, particularly the peaks of water and the methyl protons of DSS. Thus, the proposed poly-SLIC sequence acts like a singlet-state filter (*20*, *22*). This filter can be adapted to select the response of a molecule of interest. This can be achieved by using poly-SLIC excitation of delocalized LLSs in several CH_2 groups of a chosen molecule, as shown below. The probability that several methylene signals of different molecules overlap is low.

The decay curves of the four LLS signals were obtained simultaneously (Fig. 2C) so that their lifetimes T_{LLS} could be determined in parallel. The observed lifetimes T_{LLS} in different molecules in Fig. 2C range from 5.9 s for DSS to 20.6 s for taurine. Comparisons of T_{LLS} measured under the same conditions may provide insight into the stochastic fluctuations that are responsible for the relaxation of LLSs. The shortest-lived LLS in this mixture was observed in DSS, which can be explained by its slower rotational diffusion and by the presence of the $Si(CH_3)_3$ group (see Fig. 1). All nine methyl protons contribute to LLS relaxation through dipole-dipole interactions. Ethanolamine and taurine, on the other hand, have only two CH_2 groups, which contribute less to LLS relaxation.

LLS contrast in MRI experiments

Figure 3 shows the results of MRI experiments where poly-SLIC sequences were used for the excitation and reconversion of LLSs before applying gradients for phase and frequency encoding. The LLS-MRI pulse sequence used is shown in Fig. 4B. Two examples illustrate how LLSs can be used to generate contrast in MRI. In both cases, a 5-mm NMR tube with a coaxial insert was used where the two compartments were filled with different solutions.

In the first example, both the outer and inner compartments were filled with a 250 mM solution of DSS. Bovine serum albumin (BSA) was added only to the outer compartment with a concentration of 0.25 mM. For an LLS relaxation interval τ_{rel} = 0.1 s << T_{LLS}, the signal intensities in both inner and outer tubes were comparable. However, the signals from the outer compartment were attenuated when τ_{rel} was increased to 1 or 6 s (Fig. 3B). This reflects the difference of the LLS lifetimes between the inner ($T_{LLS} \approx 8$ s) and outer compartments ($T_{LLS} \approx 4$ s) due to nonselective binding of DSS to BSA. Although DSS is not a drug and BSA is not a medically relevant protein target, one observes a pronounced contrast even for a 1000:1 concentration ratio, exacerbated by nonselective binding and adhesion of BSA to glass surfaces. We did not observe any contrast in T_2-weighted MRI maps, although T_2 should be sensitive to binding in the fast-exchange regime at high fields.

This example illustrates the use of MRI for simultaneous acquisition of NMR spectra on multiple samples (*35*). Such experiments can be generalized to study a number of capillary samples that contain different drug molecules or target proteins, with different concentrations, etc. Signal enhancement by hyperpolarization might be required if the sample volumes are small. This should allow one to increase the throughput of NMR drug screening experiments.

In the second example, the outer tube contained a solution of GABA, whereas the insert contained a solution of homotaurine. Figure 3C shows the conventional ^1H NMR spectrum of this sample with overlapping signals stemming from the CH_2 groups of GABA and homotaurine near 3 ppm. Despite this overlap, a complete separation of the GABA and homotaurine signals can be achieved by using LLS-MRI with different poly-SLIC excitation schemes. This exploits the fact that not all CH_2 signals of the two molecules overlap so that a highly selective excitation can be achieved in mixtures.

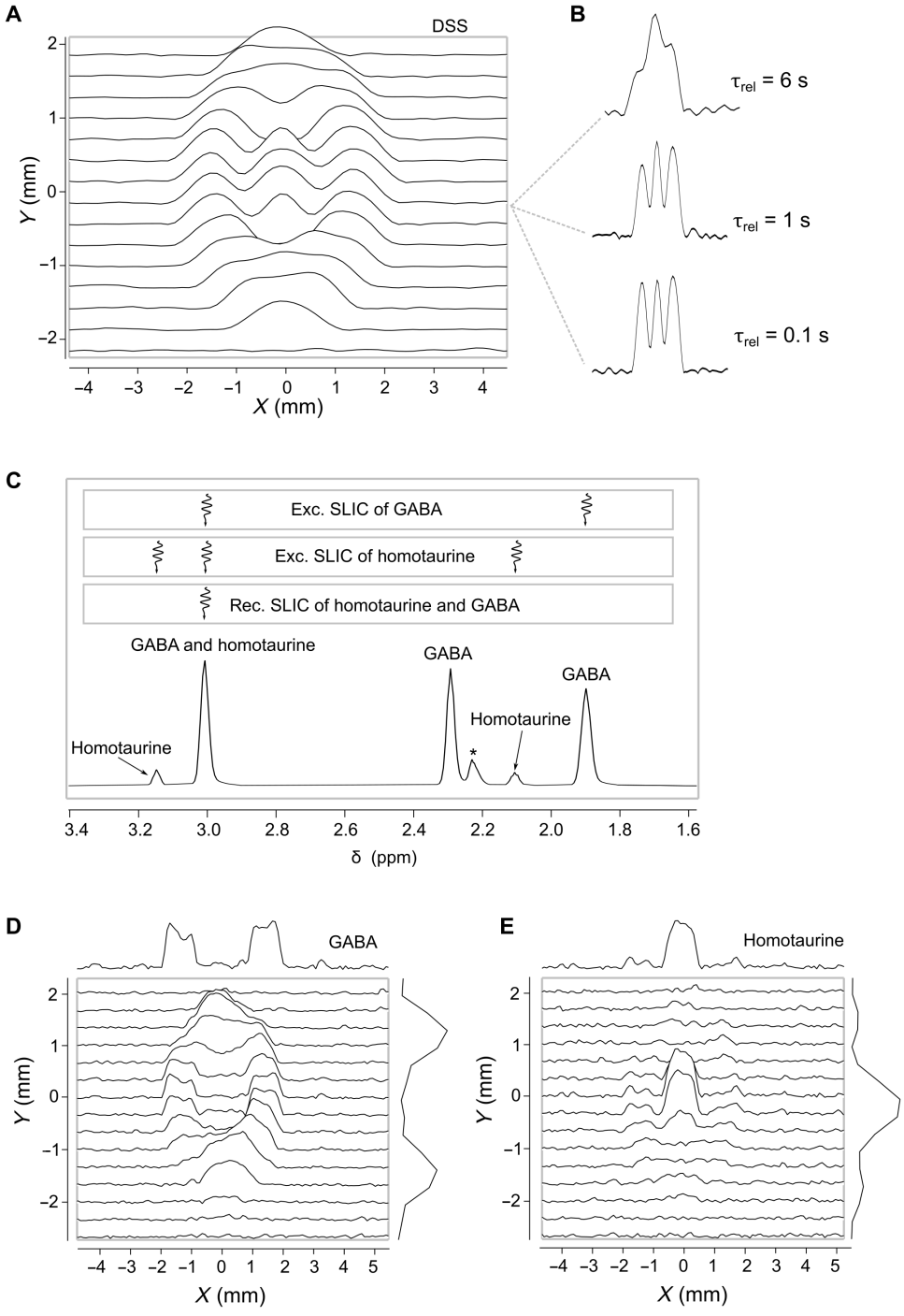

Fig. 3. LLS contrast in MRI experiments. (**A**) Axial LLS-MRI of a sample placed in two concentric tubes. Both compartments contained ca. 250 mM DSS in D_2O, but the outer compartment also contained 0.25 mM BSA. LLSs were excited by triple-SLIC and reconverted by single-SLIC after $\tau_{rel} = 0.1$ s (pulse sequence of Fig. 4B). The LLS-MRI resembles a normal MRI of this sample, because no contrast is observed for $\tau_{rel} << T_{LLS}$. (**B**) Cross sections extracted from 2D images obtained with different $\tau_{rel} = 0.1$, 1, or 6 s. The LLS-derived signal intensity decreases in the outer compartments for $\tau_{rel} = 1$ and 6 s. In the latter case, the resolution is reduced because gradient strengths G_x and G_y were decreased by a factor of 2 to improve the sensitivity. (**C**) Proton spectrum of a sample containing 1 M GABA in the outer tube and 1 M homotaurine in the inner tube. The wavy arrows indicate the frequencies used for poly-SLIC excitation and single-SLIC reconversion pulses applied at the chemical shifts of GABA and homotaurine. The RF amplitude of the excitation pulse was set to 13 Hz to fulfill both the double- and triple-SLIC conditions and excite an LLS in either GABA or homotaurine. A single-SLIC reconversion pulse with an RF amplitude of 26 Hz was applied at 3 ppm where signals of GABA and homotaurine overlap. The asterisk denotes a weak signal of acetone. (**D**) Axial MRI where an LLS was excited in GABA by double-SLIC [two wavy arrows in (C)] and reconverted by single-SLIC applied to the overlapping signal at 3 ppm. (**E**) Axial MRI where an LLS was excited in homotaurine by triple-SLIC [three wavy arrows in (C)] and reconverted by single-SLIC on the overlapping signal at 3 ppm.

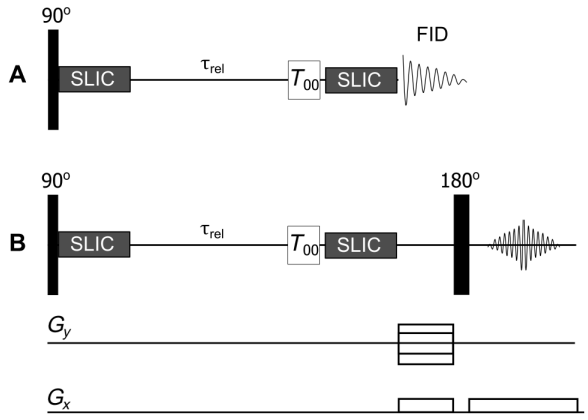

Fig. 4. SLIC pulse sequences. (**A**) Pulse sequence to study the relaxation of LLSs of one or several CH_2 groups in chains of methylene groups. A 90°$_x$ pulse is followed by a (mono- or polychromatic) SLIC pulse to excite the LLS. The second (mono- or polychromatic) SLIC pulse reconverts the LLS back to magnetization, which is then detected. The phases of the first and second SLIC pulses are alternated between *y* and *–y* together with the receiver phase (*18*). The decay of the LLS is observed by acquiring a set of 1D spectra with a variable delay trel. FID, free induction. (**B**) Combination of the SLIC pulse sequence with MRI, using phase encoding with G_y gradients that are incremented in consecutive experiments, and a G_x frequency encoding gradient to observe gradient echoes. FID, free induction decay.

DISCUSSION

LLSs involving geminal pairs of protons in CH_2 groups in achiral aliphatic chains have been excited and observed using mono- and polychromatic SLIC pulses. The lifetimes T_{LLS} of the LLSs were found to be significantly longer than T_1. This broadens the range of ligands that can be screened using LLS binding experiments. The discovery that LLSs can be excited and observed in taurine, homotaurine, GABA, dopamine, and acetylcholine opens the opportunity of combining singlet-state NMR methods with MRI to detect biologically active molecules and neurotransmitters (*52*). MRI scans of a metabolite of interest can be obtained with high molecular selectivity, as was demonstrated in LLS-MRI experiments with GABA and homotaurine. Selective excitation can be achieved by simultaneous selective irradiation of several methylene groups with chemical shifts that are characteristic for a given molecule.

It is challenging to predict in advance in which occasions the LLS will be practically inaccessible by SLIC. This depends on the rotamer populations and the associated magnitude of the magnetic inequivalence. For example, we were not successful in exciting LLSs in methylene groups of propanol, α-ketoglutarate, and serotonin. In these cases, the protons of the corresponding methylene groups were too close to magnetic equivalence. Furthermore, no LLS could be excited by SLIC in the CH_2OH groups of butanol and pentanol and in the CH_2COOH group of GABA at neutral and acidic pH.

The experimental signal amplitudes after excitation and reconversion were comparable with the theoretical calculations of the yield, provided that the effects of RF inhomogeneity ΔB_1 and T_{1rho} relaxation during the long SLIC pulses were taken into account. SLIC pulses with an adiabatic variation of the RF amplitude (*53*, *54*) can improve the performance of single-SLIC in cases where T_{1rho} of geminal protons is long enough, but the adiabatic approach is not compatible with poly-SLIC. Although adiabatic pulses are more robust with respect to B_1 inhomogeneity, they tend to be long, even for "fast" constant adiabaticity sweeps (*54*). In general, the SLIC method is superior to methods such as M2S in terms of power deposition (*25*) but more sensitive to ΔB_1 and ΔB_0 (*55*). M2S can only be used when it is applied to either *AA'* or *XX'* nuclei. When both *AA'* and *XX'* spins are simultaneously irradiated by M2S pulse trains, no LLS is created, as we observed experimentally and confirmed by simulations. M2S could be performed with selective pulses, but this would sacrifice some of its advantages with respect to SLIC. In its current version, M2S is not appropriate to convert the magnetization of both *AA'* and *XX'* pairs into LLS.

Our methodology can benefit from hyperpolarization methods such as parahydrogen-induced polarization (*56*) and signal amplification by reversible exchange (SABRE) (*57*), since aliphatic protons can often be hyperpolarized by these methods. Molecules such as dopamine and common alcohols such as butanol and pentanol, where we observed LLSs, may be hyperpolarized by SABRE or SABRE-Relay (*58*). Alternatively, dynamic nuclear polarization can be used to hyperpolarize LLSs directly, since the high temperature approximation can be violated by microwave irradiation of electron spins to bring about very low spin temperatures (*8*, *59*). Since it is not necessary to sustain the LLS by any RF irradiation, the transport of hyperpolarized samples is greatly simplified.

Our methods seek to achieve the highest possible contrast between the lifetimes T_{LLS} of a given molecule in different environments, such as a drug that is either freely tumbling in solution or partly bound to a macromolecular target such as a protein or nucleic acid, where $T_{LLS}^{bound} << T_{LLS}^{free}$, thus providing a strong contrast upon binding. This should improve titration experiments aimed at determining dissociation constants (*60*). LLSs involving protons are particularly suitable for such purposes. The contrast arises, inter alia, because the environment of achiral molecules loses its plane of symmetry upon binding to a target, i.e., the symmetry of the drug molecule is broken in the drug/target complex.

MATERIALS AND METHODS

The SLIC pulse sequence is shown in Fig. 4A. Multiple frequencies for poly-SLIC were generated by the addition of phase-modulated rectangular pulses as explained in the Supplementary Materials. To remove the spin order of ranks $0 < l \leq 3$, a single-scan T_{00} filter was used (*61*), consisting of three G_z gradient pulses, each followed by a recovery delay of 200 μs and interleaved with three nonselective 90° pulses with an RF amplitude of 10 kHz. The three gradients had sinusoidal shapes and durations of 4.4, 2.4, and 2.0 ms, while their amplitudes were set to 10, −10, and 15% of the maximum field gradient G_z = 50.05 G/cm = 0.5 T/m. The first RF pulse of the T_{00} filter, applied between the first and second gradients, had a phase ϕ = 90° (i.e., along the *y* axis), and the second and third pulses were applied after the second and third gradients, with phases ϕ = 54.7° and 0°, respectively. A four-step singlet order selection phase cycle (*18*) was used in all experiments, by alternating the phases of the excitation SLIC pulses (*y*, *–y*, *y*, *–y*) and of the reconversion SLIC pulses (*y*, *y*, *–y*, *–y*), while the phase of the receiver followed the pattern (*y*, *–y*, *–y*, *y*).

LLS experiments of strongly coupled spin pairs can be time-consuming since the recovery delays must be set to 5 T_{LLS}, unless one uses singlet order destruction filters (*62*). In this work, we have not observed any saturation effects despite using recovery delays on the order of 5 T_1, much shorter than 5 T_{LLS}. This can be explained by the low conversion yields (*63*).

NMR spectra of the individual compounds listed in Table 1 and of the mixture in Fig. 2 were obtained at 298 or 300 K with either a 5-mm iProbe or 10-mm Broad-Band Observe (BBO) probe in a Bruker 500-MHz WB magnet (B_0 = 11.66 T) equipped with a "Neo" console. The concentration of each compound in the mixture was around 10 mM. The solution was adjusted to pH 7 with 50 mM phosphate buffer in D_2O. The samples were not degassed. All poly-SLIC pulses had a common RF amplitude ν_1^{SLIC} = 27 Hz and a common duration τ_{SLIC} = 319 ms.

Monoexponential fitting was used to extract T_{LLS} relaxation times. In a few cases, a weak oscillatory behavior attributed to zero-quantum coherences was observed. The fitting was restricted to data points where such oscillations had decayed.

The MRI images were obtained without temperature stabilization at approximately 295 K in a 5-mm Micro2.5/MicWB40 probe with a Bruker 800-MHz WB system (B_0 = 18.8 T) using the pulse sequence shown in Fig. 4B. The proton linewidth was typically between 15 and 20 Hz, leading to a reduction of the yield during the highly selective SLIC pulses.

A concentric NE-5-CIC tube (Newera-spectro) with an outer diameter of 2 mm and an inner diameter of 1 mm was inserted inside a normal 5-mm NMR tube with an inner diameter of 4 mm. The first sample contained a 250 mM solution of DSS in D_2O in both the inner and outer compartments and 0.25 mM BSA (0.1%) in the outer compartment. The second sample contained a 1 M solution of GABA in D_2O in the outer compartment and a 1 M solution of homotaurine in the inner compartment. The interscan recovery delay in LLS-MRI experiments was 2 s. In the experiments carried out on the DSS sample, the G_x gradient strength was set to 4.4 G/cm, and the G_y gradient strength was linearly ramped in 16 steps from −4.4 to 4.4 G/cm. For the experiment with τ_{rel} = 6 s, all gradient strengths were decreased by a factor of 2, and the G_y gradient strength was incremented in eight steps. In all cases, 64 scans were acquired for each gradient step. In experiments with GABA and homotaurine, the same procedure was used, except that 16 scans were acquired for each step. 2D images were obtained by 2D Fourier transform with a matched sine square window function.

The Supplementary Materials additionally refer to (*64*–*66*). The raw data and Spin Dynamica (*65*) codes supporting the conclusions of the paper are available through the Zenodo repository under https://doi.org/10.5281/zenodo.7158746.

SUPPLEMENTARY MATERIALS

Supplementary material for this article is available at https://science.org/doi/10.1126/sciadv.ade2113

View/request a protocol for this paper from *Bio-protocol*.

REFERENCES AND NOTES

1. M. Carravetta, M. H. Levitt, Long-lived nuclear spin states in high-field solution NMR. *J. Am. Chem. Soc.* **126**, 6228–6229 (2004).
2. G. Pileio, J. T. Hill-Cousins, S. Mitchell, I. Kuprov, L. J. Brown, R. C. D. Brown, M. H. Levitt, Long-lived nuclear singlet order in near-equivalent ^{13}C spin pairs. *J. Am. Chem. Soc.* **134**, 17494–17497 (2012).
3. G. Stevanato, J. T. Hill-Cousins, P. Håkansson, S. S. Roy, L. J. Brown, R. C. D. Brown, G. Pileio, M. H. Levitt, A nuclear singlet lifetime of more than one hour in room-temperature solution. *Angew. Chem. Int. Ed. Engl.* **54**, 3740–3743 (2015).
4. N. Salvi, R. Buratto, A. Bornet, S. Ulzega, I. Rentero Rebollo, A. Angelini, C. Heinis, G. Bodenhausen, Boosting the sensitivity of ligand–protein screening by NMR of long-lived states. *J. Am. Chem. Soc.* **134**, 11076–11079 (2012).
5. R. Buratto, D. Mammoli, E. Chiarparin, G. Williams, G. Bodenhausen, Exploring weak ligand–protein interactions by long-lived NMR states: Improved contrast in fragment-based drug screening. *Angew. Chem. Int. Ed.* **53**, 11376–11380 (2014).
6. R. Buratto, D. Mammoli, E. Canet, G. Bodenhausen, Ligand–protein affinity studies using long-lived states of fluorine-19 nuclei. *J. Med. Chem.* **59**, 1960–1966 (2016).
7. M. B. Franzoni, L. Buljubasich, H. W. Spiess, K. Münnemann, Long-lived ^1H singlet spin states originating from para-hydrogen in Cs-symmetric molecules stored for minutes in high magnetic fields. *J. Am. Chem. Soc.* **134**, 10393–10396 (2012).
8. A. Bornet, X. Ji, D. Mammoli, B. Vuichoud, J. Milani, G. Bodenhausen, S. Jannin, Long-lived states of magnetically equivalent spins populated by dissolution-DNP and revealed by enzymatic reactions. *Eur. J. Chem.* **20**, 17113–17118 (2014).
9. K. Shen, A. W. J. Logan, J. F. P. Colell, J. Bae, G. X. Ortiz, T. Theis, W. S. Warren, S. J. Malcolmson, Q. Wang, Diazirines as potential molecular imaging tags: Probing the requirements for efficient and long-lived SABRE-induced hyperpolarization. *Angew. Chem. Int. Ed. Engl.* **56**, 12112–12116 (2017).
10. J.-B. Hövener, A. N. Pravdivtsev, B. Kidd, C. R. Bowers, S. Glöggler, K. V. Kovtunov, M. Plaumann, R. Katz-Brull, K. Buckenmaier, A. Jerschow, F. Reineri, T. Theis, R. V. Shchepin, S. Wagner, P. Bhattacharya, N. M. Zacharias, E. Y. Chekmenev, Parahydrogen-based hyperpolarization for biomedicine. *Angew. Chem. Int. Ed. Engl.* **57**, 11140–11162 (2018).
11. C. Bengs, L. Dagys, G. A. I. Moustafa, J. W. Whipham, M. Sabba, A. S. Kiryutin, K. L. Ivanov, M. H. Levitt, Nuclear singlet relaxation by chemical exchange. *J. Chem. Phys.* **155**, 124311 (2021).
12. S. Cavadini, J. Dittmer, S. Antonijevic, G. Bodenhausen, Slow diffusion by singlet state NMR spectroscopy. *J. Am. Chem. Soc.* **127**, 15744–15748 (2005).
13. M. C. Tourell, I.-A. Pop, L. J. Brown, R. C. D. Brown, G. Pileio, Singlet-assisted diffusion-NMR (SAD-NMR): Redefining the limits when measuring tortuosity in porous media. *Phys. Chem. Chem. Phys.* **20**, 13705–13713 (2018).
14. P. R. Vasos, A. Comment, R. Sarkar, P. Ahuja, S. Jannin, J.-P. Ansermet, J. A. Konter, P. Hautle, B. van den Brandt, G. Bodenhausen, Long-lived states to sustain hyperpolarized magnetization. *Proc. Natl. Acad. Sci. U.S.A.* **106**, 18469–18473 (2009).
15. T. Theis, G. X. Ortiz, A. W. J. Logan, K. E. Claytor, Y. Feng, W. P. Huhn, V. Blum, S. J. Malcolmson, E. Y. Chekmenev, Q. Wang, W. S. Warren, Direct and cost-efficient hyperpolarization of long-lived nuclear spin states on universal $^{15}N_2$-diazirine molecular tags. *Sci. Adv.* **2**, e1501438 (2016).
16. S. S. Roy, P. Norcott, P. J. Rayner, G. G. R. Green, S. B. Duckett, A hyperpolarizable ^1H magnetic resonance probe for signal detection 15 minutes after spin polarization storage. *Angew. Chem. Int. Ed. Engl.* **55**, 15642–15645 (2016).
17. B. Procacci, S. S. Roy, P. Norcott, N. Turner, S. B. Duckett, Unlocking a diazirine long-lived nuclear singlet state via photochemistry: NMR detection and lifetime of an unstabilized diazo-compound. *J. Am. Chem. Soc.* **140**, 16855–16864 (2018).
18. A. S. Kiryutin, A. N. Pravdivtsev, A. V. Yurkovskaya, H.-M. Vieth, K. L. Ivanov, Nuclear spin singlet order selection by adiabatically ramped RF fields. *J. Phys. Chem. B* **120**, 11978–11986 (2016).
19. S. Mamone, N. Rezaei-Ghaleh, F. Opazo, C. Griesinger, S. Glöggler, Singlet-filtered NMR spectroscopy. *Sci. Adv.* **6**, eaaz1955 (2020).
20. J. Eills, E. Cavallari, R. Kircher, G. D. Matteo, C. Carrera, L. Dagys, M. H. Levitt, K. L. Ivanov, S. Aime, F. Reineri, K. Münnemann, D. Budker, G. Buntkowsky, S. Knecht, Singlet-contrast magnetic resonance imaging: Unlocking hyperpolarization with metabolism. *Angew. Chem. Int. Ed. Engl.* **60**, 6791–6798 (2021).
21. A. S. Kiryutin, H. Zimmermann, A. V. Yurkovskaya, H.-M. Vieth, K. L. Ivanov, Long-lived spin states as a source of contrast in magnetic resonance spectroscopy and imaging. *J. Magn. Reson.* **261**, 64–72 (2015).
22. C. Huang, Y. Peng, E. Lin, Z. Ni, X. Lin, H. Zhan, Y. Huang, Z. Chen, Adaptable singlet-filtered nuclear magnetic resonance spectroscopy for chemical and biological applications. *Anal. Chem.* **94**, 4201–4208 (2022).
23. M. H. Levitt, Long live the singlet state! *J. Magn. Reson.* **306**, 69–74 (2019).
24. M. C. D. Tayler, M. H. Levitt, Singlet nuclear magnetic resonance of nearly-equivalent spins. *Phys. Chem. Chem. Phys.* **13**, 5556–5560 (2011).
25. S. J. DeVience, R. L. Walsworth, M. S. Rosen, Preparation of nuclear spin singlet states using spin-lock induced crossing. *Phys. Rev. Lett.* **111**, 173002 (2013).
26. Y. Feng, R. M. Davis, W. S. Warren, Accessing long-lived nuclear singlet states between chemically equivalent spins without breaking symmetry. *Nat. Phys.* **8**, 831–837 (2012).
27. Y. Feng, T. Theis, X. Liang, Q. Wang, P. Zhou, W. S. Warren, Storage of hydrogen spin polarization in long-lived $^{13}C_2$ singlet order and implications for hyperpolarized magnetic resonance imaging. *J. Am. Chem. Soc.* **135**, 9632–9635 (2013).
28. Y. Feng, T. Theis, T.-L. Wu, K. Claytor, W. S. Warren, Long-lived polarization protected by symmetry. *J. Chem. Phys.* **141**, 134307 (2014).
29. K. Claytor, T. Theis, Y. Feng, J. Yu, D. Gooden, W. S. Warren, Accessing long-lived disconnected spin-1/2 eigenstates through spins > 1/2. *J. Am. Chem. Soc.* **136**, 15118–15121 (2014).
30. K. F. Sheberstov, H.-M. Vieth, H. Zimmermann, B. A. Rodin, K. L. Ivanov, A. S. Kiryutin, A. V. Yurkovskaya, Generating and sustaining long-lived spin states in $^{15}N,^{15}N'$-azobenzene. *Sci. Rep.* **9**, 20161 (2019).

31. S. Yang, P. Saul, S. Mamone, L. Kaltschnee, S. Glöggler, Bimodal fluorescence/magnetic resonance molecular probes with extended spin lifetimes. *Eur. J. Chem.* **28**, e202104158 (2022).
32. Z. Zhou, K. Claytor, W. S. Warren, T. Theis, Accessing long lived ^{1}H states via ^{2}H couplings. *J. Magn. Reson.* **263**, 108–115 (2016).
33. G. Pileio, M. H. Levitt, J-stabilization of singlet states in the solution NMR of multiple-spin systems. *J. Magn. Reson.* **187**, 141–145 (2007).
34. Y. Kim, M. Liu, C. Hilty, Parallelized ligand screening using dissolution dynamic nuclear polarization. *Anal. Chem.* **88**, 11178–11183 (2016).
35. A. Ross, G. Schlotterbeck, H. Senn, M. von Kienlin, Application of chemical shift imaging for simultaneous and fast acquisition of NMR spectra on multiple samples. *Angew. Chem. Int. Ed.* **40**, 3243–3245 (2001).
36. G. Pileio, M. Carravetta, M. H. Levitt, Storage of nuclear magnetization as long-lived singlet order in low magnetic field. *Proc. Natl. Acad. Sci. U.S.A.* **107**, 17135–17139 (2010).
37. M. Sabba, N. Wili, C. Bengs, L. J. Brown, M. H. Levitt, Symmetry-based singlet-triplet excitation in solution nuclear magnetic resonance. *J. Chem. Phys.* **157**, 134302 (2022).
38. G. Stevanato, Alternating Delays Achieve Polarization Transfer (ADAPT) to heteronuclei in PHIP experiments. *J. Magn. Reson.* **274**, 148–162 (2017).
39. J. Eills, G. Stevanato, C. Bengs, S. Glöggler, S. J. Elliott, J. Alonso-Valdesueiro, G. Pileio, M. H. Levitt, Singlet order conversion and parahydrogen-induced hyperpolarization of ^{13}C nuclei in near-equivalent spin systems. *J. Magn. Reson.* **274**, 163–172 (2017).
40. G. Stevanato, J. Eills, C. Bengs, G. Pileio, A pulse sequence for singlet to heteronuclear magnetization transfer: S2hM. *J. Magn. Reson.* **277**, 169–178 (2017).
41. Y. Ding, S. Korchak, S. Mamone, A. P. Jagtap, G. Stevanato, S. Sternkopf, D. Moll, H. Schroeder, S. Becker, A. Fischer, E. Gerhardt, T. F. Outeiro, F. Opazo, C. Griesinger, S. Glöggler, Rapidly signal-enhanced metabolites for atomic scale monitoring of living cells with magnetic resonance. *Chemistry–Methods* **2**, e202200023 (2022).
42. S. J. DeVience, R. L. Walsworth, M. S. Rosen, Probing scalar coupling differences via long-lived singlet states. *J. Magn. Reson.* **262**, 42–49 (2016).
43. S. J. DeVience, M. Greer, S. Mandal, M. S. Rosen, Homonuclear J-coupling spectroscopy at low magnetic fields using spin-lock induced crossing. *ChemPhysChem* **22**, 2128–2137 (2021).
44. D. A. Barskiy, O. G. Salnikov, A. S. Romanov, M. A. Feldman, A. M. Coffey, K. V. Kovtunov, I. V. Koptyug, E. Y. Chekmenev, NMR spin-lock induced crossing (SLIC) dispersion and long-lived spin states of gaseous propane at low magnetic field (0.05 T). *J. Magn. Reson.* **276**, 78–85 (2017).
45. A. Sonnefeld, G. Bodenhausen, K. Sheberstov, Polychromatic excitation of delocalized long-lived proton spin states in aliphatic chains. *Phys. Rev. Lett.* **129**, 183203 (2022).
46. J. A. Pople, W. G. Schneider, H. J. Bernstein, The analysis of nuclear magnetic resonance spectra: II. Two pairs of two equivalent nuclei. *Can. J. Chem.* **35**, 1060–1072 (1957).
47. K. G. R. Pachler, P. L. Wessels, Rotational isomerism: V. A nuclear magnetic resonance study of 1,2-diiodoethane. *J. Mol. Struct.* **3**, 207–218 (1969).
48. M. J. Minch, Orientational dependence of vicinal proton-proton NMR coupling constants: The Karplus relationship. *Concepts Magn. Reson.* **6**, 41–56 (1994).
49. H. J. Hogben, P. J. Hore, I. Kuprov, Multiple decoherence-free states in multi-spin systems. *J. Magn. Reson.* **211**, 217–220 (2011).
50. O. W. Sørensen, Polarization transfer experiments in high-resolution NMR spectroscopy. *Prog. Nucl. Magn. Reson. Spectrosc.* **21**, 503–569 (1989).
51. M. H. Levitt, Symmetry constraints on spin dynamics: Application to hyperpolarized NMR. *J. Magn. Reson.* **262**, 91–99 (2016).
52. T. Lee, L. X. Cai, V. S. Lelyveld, A. Hai, A. Jasanoff, Molecular-level functional magnetic resonance imaging of dopaminergic signaling. *Science* **344**, 533–535 (2014).
53. T. Theis, Y. Feng, T. Wu, W. S. Warren, Composite and shaped pulses for efficient and robust pumping of disconnected eigenstates in magnetic resonance. *J. Chem. Phys.* **140**, 014201 (2014).
54. B. A. Rodin, K. F. Sheberstov, A. S. Kiryutin, J. T. Hill-Cousins, L. J. Brown, R. C. D. Brown, B. Jamain, H. Zimmermann, R. Z. Sagdeev, A. V. Yurkovskaya, K. L. Ivanov, Constant-adiabaticity radiofrequency pulses for generating long-lived singlet spin states in NMR. *J. Chem. Phys.* **150**, 064201 (2019).
55. B. Kharkov, X. Duan, J. W. Canary, A. Jerschow, Effect of convection and B_1 inhomogeneity on singlet relaxation experiments. *J. Magn. Reson.* **284**, 1–7 (2017).
56. C. R. Bowers, D. P. Weitekamp, Parahydrogen and synthesis allow dramatically enhanced nuclear alignment. *J. Am. Chem. Soc.* **109**, 5541–5542 (1987).
57. R. W. Adams, J. A. Aguilar, K. D. Atkinson, M. J. Cowley, P. I. P. Elliott, S. B. Duckett, G. G. R. Green, I. G. Khazal, J. López-Serrano, D. C. Williamson, Reversible interactions with para-hydrogen enhance NMR sensitivity by polarization transfer. *Science* **323**, 1708–1711 (2009).
58. W. Iali, P. J. Rayner, S. B. Duckett, Using *para*hydrogen to hyperpolarize amines, amides, carboxylic acids, alcohols, phosphates, and carbonates. *Sci. Adv.* **4**, eaao6250 (2018).
59. M. C. D. Tayler, I. Marco-Rius, M. I. Kettunen, K. M. Brindle, M. H. Levitt, G. Pileio, Direct enhancement of nuclear singlet order by dynamic nuclear polarization. *J. Am. Chem. Soc.* **134**, 7668–7671 (2012).
60. A. D. Gossert, W. Jahnke, NMR in drug discovery: A practical guide to identification and validation of ligands interacting with biological macromolecules. *Prog. Nucl. Magn. Reson. Spectrosc.* **97**, 82–125 (2016).
61. M. C. D. Tayler, Chapter 10: Filters for Long-lived Spin Order, in *Long-lived Nuclear Spin Order* (The Royal Society of Chemistry, 2020), pp. 188–208.
62. B. A. Rodin, K. F. Sheberstov, A. S. Kiryutin, L. J. Brown, R. C. D. Brown, M. Sabba, M. H. Levitt, A. V. Yurkovskaya, K. L. Ivanov, Fast destruction of singlet order in NMR experiments. *J. Chem. Phys.* **151**, 234203 (2019).
63. B. A. Rodin, C. Bengs, A. S. Kiryutin, K. F. Sheberstov, L. J. Brown, R. C. D. Brown, A. V. Yurkovskaya, K. L. Ivanov, M. H. Levitt, Algorithmic cooling of nuclear spins using long-lived singlet order. *J. Chem. Phys.* **152**, 164201 (2020).
64. G. Stevanato, S. S. Roy, J. Hill-Cousins, I. Kuprov, L. J. Brown, R. C. D. Brown, G. Pileio, M. H. Levitt, Long-lived nuclear spin states far from magnetic equivalence. *Phys. Chem. Chem. Phys.* **17**, 5913–5922 (2015).
65. C. Bengs, M. H. Levitt, SpinDynamica: Symbolic and numerical magnetic resonance in a Mathematica environment. *Magn. Reson. Chem.* **56**, 374–414 (2018).
66. K. F. Sheberstov, A. S. Kiryutin, C. Bengs, J. T. Hill-Cousins, L. J. Brown, R. C. D. Brown, G. Pileio, M. H. Levitt, A. V. Yurkovskaya, K. L. Ivanov, Excitation of singlet–triplet coherences in pairs of nearly-equivalent spins. *Phys. Chem. Chem. Phys.* **21**, 6087–6100 (2019).

Acknowledgments: We are indebted to U. le Paige and N. Birlirakis for stimulating discussions. **Funding:** We acknowledge the CNRS and ENS for support and the European Research Council (ERC) for the Synergy grant "Highly Informative Drug Screening by Overcoming NMR Restrictions" (HISCORE, grant agreement number 951459). **Author contributions:** Conceptualization: K.S. and G.B. Methodology: A.S. and K.S. Software: K.S. Formal analysis: A.S., A.R., and K.S. Investigation: A.S., A.R., P.P., and K.S. Visualization: A.S. and K.S. Writing—original draft: A.S., G.B., and K.S. Writing—review and editing: A.S., P.P., G.B., and K.S. Supervision: G.B and P.P. Funding acquisition: G.B. **Competing interests:** The authors declare that they have no competing interests. **Data and materials availability:** All data needed to evaluate the conclusions in the paper are present in the paper and/or the Supplementary Materials.

Submitted 1 August 2022
Accepted 19 October 2022
Published 2 December 2022
10.1126/sciadv.ade2113

Long-lived states of methylene protons in achiral molecules

Anna SonnefeldAiky RazanahoeraPhilippe PelupessyGeoffrey BodenhausenKirill Sheberstov

Sci. Adv., 8 (48), eade2113. • DOI: 10.1126/sciadv.ade2113

Science Advances (ISSN) is published by the American Association for the Advancement of Science. 1200 New York Avenue NW, Washington, DC 20005. The title *Science Advances* is a registered trademark of AAAS.